We are IntechOpen, the world's leading publisher of Open Access books Built by scientists, for scientists

4,800
Open access books available

122,000
International authors and editors

135M
Downloads

Our authors are among the

154
Countries delivered to

TOP 1%
most cited scientists

12.2%
Contributors from top 500 universities

CLARIVATE ANALYTICS BOOK CITATION INDEX INDEXED

WEB OF SCIENCE™

Selection of our books indexed in the Book Citation Index in Web of Science™ Core Collection (BKCI)

Interested in publishing with us?
Contact book.department@intechopen.com

Numbers displayed above are based on latest data collected.
For more information visit www.intechopen.com

14

Contrast Improvement of Relativistic Few-Cycle Light Pulses

László Veisz
Max-Planck-Institut für Quantenoptik
Germany

1. Introduction

Laser-plasma interaction has been a widespread and popular field of research since the birth of the laser. It involves numerous interesting phenomena such as inertial confinement fusion; generation and acceleration of electron, positron, neutron, proton and ion particle beams; source of electro-magnetic radiation in the IR, visible, UV and x-ray range, just to mention some important applications. The continuously increasing power and the development of chirped pulse amplification lead to electric fields in which oscillating free electrons reach almost the speed of light. This so called relativistic optics regime starts at intensities about 10^{18} W/cm^2 at 1 μm wavelength. The interaction of relativistically intense laser pulses with solid state -possibly liquid- target material is always accompanied by the creation of inhomogeneous plasmas, as a given amount of extended preplasma is formed in front of the target before the main laser pulse arrives. This preplasma is produced by undesired laser light impinging onto the target before the short main pulse. Its density decreases rapidly farther from the target due to the hydrodynamic expansion of the hot plasma during the time till the interaction pulse comes. The extension of the preplasma significantly influences the interaction and leads to completely different types of processes depending on its value. Typical lasers produce an extended preplasma before the main pulse, because they amplify pre- and postpulses and pedestals from various origins. Therefore a certain types of processes involving interaction of intense laser pulse with extended low density plasmas dominate these investigations. On the other hand, practically preplasma-free environment is required by various relativistic laser-plasma experiments involving ultra-intense laser and high-density plasma interaction like surface high harmonic generation Monot et al. (2004); Thaury et al. (2007), laser-driven proton and ion acceleration Hegelich et al. (2006) or laser interaction with few nanometer thick diamond-like-carbon foils, so called nanofoils. This preplasma formation is influenced by the contrast, which characterizes the laser intensity before and after the main pulse relative to this pulse. Therefore precise characterization and improvement of the contrast are essential to successfully conduct these types of experiments.
Laser pulses with a duration of only a few optical cycles at moderate intensities opened up the new era of attosecond physics Brabec & Krausz (2000); Krausz & Ivanov (2009) via the controlled reproducible generation of weak XUV pulses with a duration of hundred(s) of attoseconds precisely synchronized to the laser pulse. These pulses allow the investigation of electron motion in atoms, molecules and solid states in an XUV pump and visible / near infrared probe configuration. Relativistic intensity few-cycle sources hold the promise to generate XUV pulses with unprecedented energy and thus form the basis of the novel research

field of XUV pump XUV probe investigations with single attosecond bursts.
This chapter concentrates on the contrast enhancement of few-cycle light sources. The main topics discussed are the characterization of laser contrast, implementation and application of contrast enhancement techniques. It should be noted already here that these methods are perfectly suited for longer -from many optical cycle long up to picosecond- laser pulses as well. Two successful and efficient techniques, the plasma mirror and the optical parametric (chirped pulse) amplification, were applied for the generation of few-cycle pulses with extreme contrast. The first section starts with the introduction of the most important physical quantities and overview of the various techniques followed by a description of the above mentioned two methods and also the cross-polarized wave generation (XPW). This section closes with the description of contrast measurement techniques. The results in the next section present realization, characterization and some practical tips to contrast enhancement. Discussion, future work and conclusions are at the end of this chapter.

2. Overview and methods

In the first part of this section the most important parameters are summarized and quantified relevant to the characterization of the high-dynamic range contrast of ultrahigh-intensity laser systems and the contrast requirements by experiments are discussed. Thereafter the most general contrast enhancement techniques are shortly introduced with their advantages and shortcomings.

2.1 Overview of the important physical phenomena

The interaction of relativistic intensity - $I \geq 10^{18}$ W/cm^2 - laser pulses with solid or liquid targets results in the ionization of the target material much before the main intense pulse, changing the plasma properties and the interaction itself as mentioned in the introduction. The generated plasma is heated rapidly to hot temperatures and starts to expand creating typically an exponential plasma density ramp in front of the target as shown in Fig. 1. A fully ionized solid state target has a maximal electron plasma density (n_{max}) of about 10^{24} cm^{-3}.

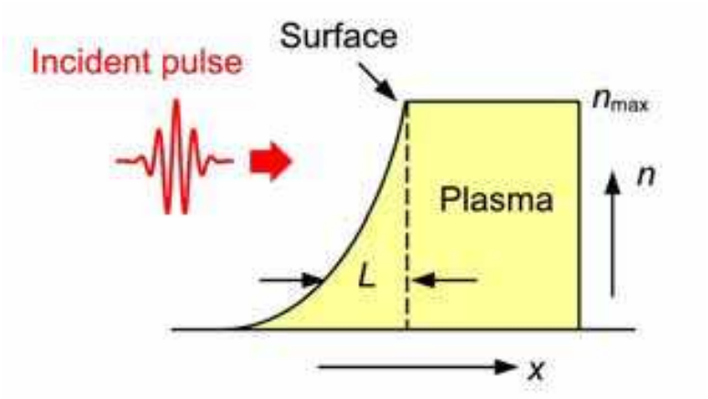

Fig. 1. Typical plasma density (n) from laser irradiated solid state or liquid targets as a function of the perpendicular coordinate to the surface (x). As the maximal electron density (n_{max}) corresponding to the solid density is much higher than the critical density, the light is reflected and interacts with the preplasma characterized by its extension (L), the so-called electron density scale length.

The critical density -where the plasma frequency reaches the laser frequency- is a very specific electron density:

$$n_c = \omega_0^2 m_e \varepsilon_0 / e^2; \qquad n_c(cm^{-3}) = 1.1 \times 10^{21} \lambda^{-2}(\mu m) \tag{1}$$

where $\lambda, \omega_0 = 2\pi c/\lambda$ are the laser wavelength and frequency, c is the speed of light in vacuum, ε_0 is the vacuum permittivity and $2m_e$, e are the electron mass and charge, respectively. The critical density has a value of 1.7×10^{21} cm^{-3} at $\lambda = 800$ nm laser wavelength indicating that the plasma near to a typical target gets a few 100 times "overdense" which means that the plasma density correspondingly exceeds the critical density. The light propagating in an inhomogeneous plasma upward the density gradient is reflected and partially absorbed at the critical density depending on the preplasma extension and cannot penetrate deeper to even higher densities Kruer (1988). The preplasma extension has an important role and it is characterized by the so-called *electron plasma density scale length*:

$$L = \left| n_e \left(\frac{dn_e}{dx} \right)^{-1} \right|_{x_0} \tag{2}$$

which is generally taken at the critical density ($x_0 = x_{cr}$). It is usual to normalize this value to the laser wavelength as this is the real physical measure of the plasma. The laser electric field is evanescent in the overdense plasma and its penetration, i.e. how high densities will the laser light reach, is characterized by this normalized quantity. Typically a normalized scale length of 0.1 is a good value allowing efficient implementation of surface high harmonic generation or ion acceleration, around 1 it is an average value suppressing / prohibiting the previous experiments and significantly higher than 1 is poor value involving mainly laser interaction with underdense plasmas like in gas targets and generation of electrons and bremsstrahlung. The normalized density scale length depends on the target material and the temporal structure and amount of laser light impinging onto the target before the main pulse. The high-dynamic-range temporal structure of laser light is described by the contrast, which is defined by the ratio of the laser main pulse intensity to the intensity at a given time instant. The reciprocal value is also used as contrast for example in the autocorrelation measurement. Fig. 2. depicts a typical temporal structure of ultrahigh intensity laser pulses. Sources that generate these pulses are based on the principle of chirped pulse amplification (CPA) Strickland & Mourou (1985); Yanovsky et al. (2008) or optical parametric chirped pulse amplification (OPCPA) systems Herrmann et al. (2009); Lozhkarev et al. (2007); Hernandez-Gomez et al. (2010). The temporal structure contains pedestals -long background pulses of different duration-, pre- and postpulses -short weak pulses- and the "foot" of the main laser pulse. Nanosecond pedestals with a contrast of 10^{-5} to 10^{-8} -or 5 to 8 orders of magnitude- can for example originate from amplified spontaneous emission (ASE) in the CPA laser amplifier; while the pre- and postpulses with typically 2 to 6 orders of magnitude contrast come from birefringence of optical elements, double internal reflections in optics or amplification of a previous oscillator / regenerative amplifier pulses and have temporal distance of a few 100 fs to many ns to the main pulse. A typical source of the foot of the pulse with 3 to 6 orders of magnitude contrast is the imperfect compression, but the noisy spectrum itself from amplification might also be a source.

The damage threshold is approximately the start of irreversible processes and plasma formation. It depends on the target material and laser pulse duration and varies from 10^{10} W/cm^2 for ns pulses to 10^{13} W/cm^2 for fs pulses in dielectrics Stuart et al. (1995; 1996); Tien et al. (1999) and it can reach even lower values for metals and liquids.

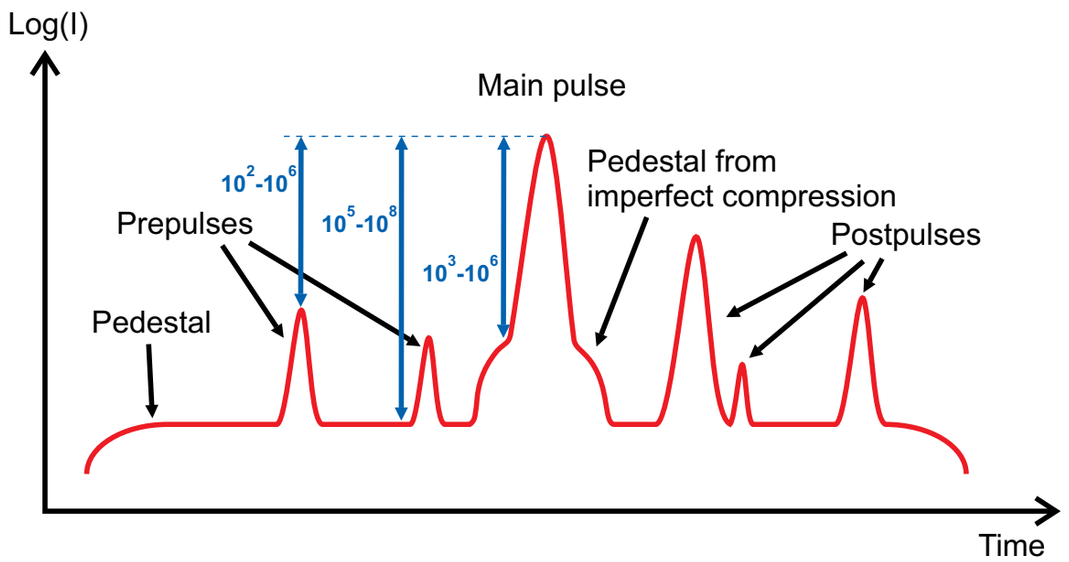

Fig. 2. Typical temporal structure of a laser pulse from a chirped-pulse amplification (CPA) or optical parametric chirped pulse amplification (OPCPA) system. Aside from the main pulse, it generally has pre- and postpulses. Pedestals usually arise from amplified spontaneous emission (ASE) and imperfect compression. Contrast of the pulse is defined by the ratio between the intensities of the main pulse and prepulses/pedestal. Typical values of the contrast are indicated for prepulses and pedestals.

Correspondingly, $10^{-8} - 10^{-12}$ contrast is required for preplasma sensitive experiments with presently reachable peak intensities of $10^{18} - 10^{22}$ W/cm^2 Yanovsky et al. (2008). The current demand of typically 8 - 12 orders of magnitude contrast on laser systems is already very high. Future multi-PW systems have even more enormous expectations of 12 - 14 orders of magnitude contrast and in the same time an ultra-broad bandwidth requirement supporting even few-cycle pulse duration. Nowadays widespread chirped pulse amplification (CPA) lasers and newly appearing optical parametric chirped pulse amplification (OPCPA) systems without extra contrast improvement technology are not capable to fulfill these requirements.

2.2 Summary of the relevant technologies

As the required contrast is higher than the typically available one various *contrast enhancement techniques* have been developed. Here we shortly summarize the most known methods that can be divided into three categories. The first category contains various approaches that work with only a limited input energy -on the order of 1 mJ- and have relative low conversion efficiency -generally 10%-, but enhance the contrast by a higher value -from 3 to 9 orders of magnitude maximal improvement. These techniques are not applicable to the final laser output due to their limitations therefore they are applied in a double chirped pulse amplification scheme Kalashnikov et al. (2005), where after the first amplifiers the pulses are compressed cleaned and later stretched, amplified and compressed a second time. The following approaches belong to this category:

– non-linear Sagnac interferometer Renault et al. (2005). It applies a Sagnac interferometer -containing a beam splitter and two mirrors- a filter and a Kerr nonlinear medium. The efficiency is about 10-20 %, contrast enhancement is 4 order of magnitude (OOM), the quality of output profile is decreased.

– saturable absorber Itatani et al. (1998); Kiriyama et al. (2010), is applied after some preamplifier stages at the μJ energy level in compressed pulses with $\sim$ 20% efficiency. The contrast is bettered by only 2 OOM.
– elliptical polarization rotation in air Homoelle et al. (2002); Jullien et al. (2004); Kalashnikov et al. (2004) is based on the nonlinear induced birefringence. The efficiency is 25-50 % depending on the configuration -single vs. multi pass- and on the chirp of the input pulse and the contrast enhancement is 3-4 OOM. The stability of the output pulses is reduced.
– cross-polarized wave generation Jullien et al. (2005); Chvykov et al. (2006). This technique is discussed in more detail in the next section.
– self-diffraction process in a Kerr nonlinear medium Liu & Kobayashi (2010) was suggested as this third order nonlinearity generates the cleaned beam propagating in a new different direction than the input beams. It has about 10 % efficiency and an improvement of 4.5 OOM corresponding to cubic temporal intensity dependence has been demonstrated with a potential of even better values.

The second category of contrast enhancement techniques have no input energy limitation, have higher efficiency -in the range of 35-80%- and consequently are applicable at the end of the laser systems. Therefore they improve the contrast on target, i.e. prepulses and pedestals even from compression is improved. The drawback of these approaches is that their efficiency influences directly the final energy of the system and it cannot be regained by further amplification. One of the oldest idea to improve the contrast is the frequency doubling of the pulses Marcinkevičius et al. (2004); Yuan et al. (2010). Theoretically the contrast is squared applying frequency doubling in typically KDP crystals, but the energy conversion efficiency is limited (35%-80%), the quality of the beam profile and wavefront is decreased. The effort to increase the efficiency requires thick crystals that limit the bandwidth and so the lowest pulse duration to above approx. 100 fs and reduces the contrast improvement around the main pulse. Plasma mirrors in a single / double configuration are another example of this category having 70 / 50% efficiency, 2-3 orders of magnitude improvement and better spatial beam profile.
The third category includes the optical parametric amplification (OPA) and optical parametric chirped pulse amplification (OPCPA) based methods. They are connected to the amplification and are not dedicated only to the contrast and so are not always classified in the two previous categories. The following examples are based on OP(CP)A:

– OP(CP)A preamplifier stage is used for idler generation Shah et al. (2009); Lozhkarev et al. (2006). At the beginning of a ultrahigh-intensity system a non-collinear OPA / OPCPA stage is installed. The idler is used for further amplification from this stage, which is not generated just when the pump and the seed are also present. Very high contrast improvement factors are realized, but the angular chirp must be (pre-)compensated and so it is not practical for few-cycle pulses.
– non-saturated OP(CP)A preamplifier stage substituting complex laser amplifiers in hybrid OPCPA CPA laser systems Gaul et al. (2010); Kiriyama et al. (2008). This technique applying typically a nanosecond pump laser is generally not improving the contrast just preserving a good input value and substitutes a large laser preamplifiers that reduce the contrast.
– OPCPA system with short pump pulse duration (from 1 ps up to $\sim$100 ps) Herrmann et al. (2009); Gu et al. (2009); Major et al. (2009); Dorrer et al. (2007). This technique is discussed in more detail in the next section.

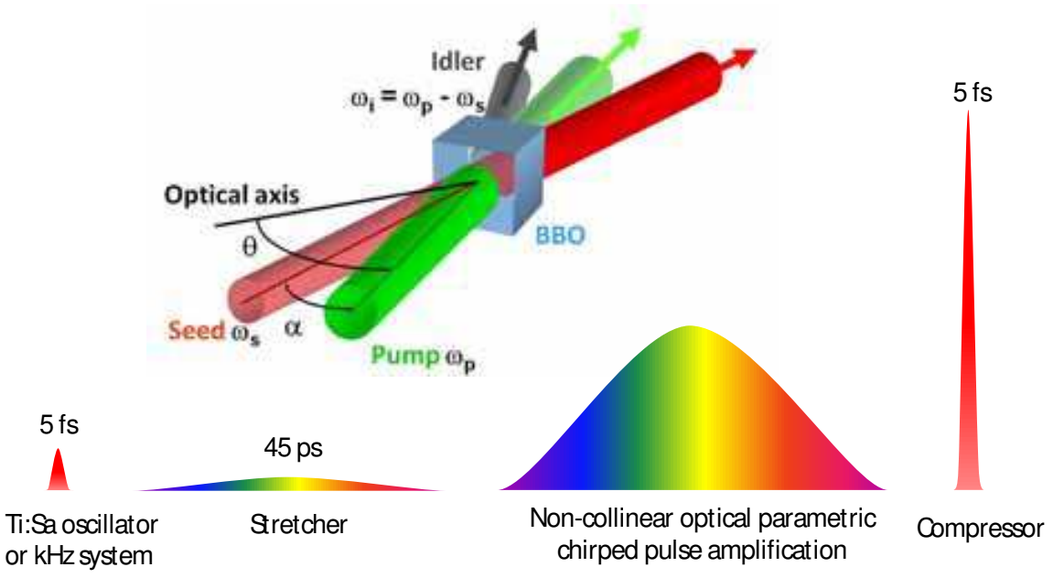

Fig. 3. Schematics of an optical parametric chirped pulse amplification system. The short and weak pulses from a Ti:sapphire oscillator or multipass amplifier are stretched in time, amplified via noncollinear OPCPA with "short" pump pulses and compressed in a suitable stretcher. Inset: basic setup of an OP(CP)A stage with the weak input seed, strong and short input pump and the generated amplified signal and idler.

A lot of strategies were developed to improve the contrast as listed above, but their applicability to few-cycle light sources was not or rarely investigated. After this summary of the contrast enhancement techniques two of them applied -and one planned to be applied- in our few-cycle systems are discussed in more detail.

2.2.1 Optical parametric amplification and optical parametric chirped pulse amplification

The goal of this section is to introduce the basic principles of optical parametric amplification (OPA) and optical parametric chirped pulse amplification (OPCPA) schemes and show their advantage in contrast enhancement. It is far from a complete description of these approaches. For more complete reviews see Refs. Cerullo & De Silvestri (2003); Dubietis et al. (2006). OPA is a second order nonlinear process in which from an input beam called pump, energy is transferred to another input beam called signal and as a byproduct a third output beam called idler at the difference frequency of the pump and the signal frequency is generated as shown in Fig. 3 inset. This parametric amplification process of the signal is taking place in nonlinear optical crystals such as BBO, LBO, KDP, etc. and is characterized by phase matching -originating from momentum conservation- between the three involved waves which determines the spectral bandwidth and decreases with increasing crystal thickness and an exponential amplification of the signal wave. The nonsaturated gain is proportional to the crystal thickness and the root of the pump intensity -the amplification is an exponential function of the gain. OPCPA Dubietis et al. (1992) is a technique, where a short signal pulse, generated for example by a Titanium:sapphire oscillator or a kHz amplifier, is stretched temporally to match the pump pulse duration. Thereafter a -typically- noncollinear OPA stage with the chirped pulses -termed OPCPA stage- amplifies the pulses that are compressed at the end of the system as shown in Fig. 3.

The OPCPA has various advantages over conventional laser amplifiers:

– Very broad gain bandwidth reaching ¿300 nm, which is not available from conventional amplification by lasers. This supports pulses with few optical cycle duration.
– Huge single pass gain reaching a value of 10^6. However typically much lower gain values are used to preserve the good contrast.
– Negligible thermal load in the amplifier crystals in contrary to laser amplifiers. No cooling is needed, which is one of the biggest challenges in lasers.
– Good contrast achievable if the pump pulse is relative short (1 ps to $\sim$100 ps) as the gain exists only during the short pump pulse. Any kind of signal -as stretched seed or undesired background- is correspondingly only amplified in the temporal window of the pump.

The following challenges are connected to OPCPA:

– Stretching and compression of huge spectral bandwidth -relevant mainly for few-cycle pulses- with a precise spectral phase control and high compressor throughput. These expectations limit the stretching ratio.
– The pump laser easily becomes a complex system when its duration is much shorter than a few nanosecond duration of commercially available sources. The short pump duration is required due to the limited stretching and the good required contrast of signal.
– Synchronization of pump and seed is getting difficult with decreasing pump pulse duration, requiring special techniques as optical synchronization Teisset et al. (2005) or even active delay stabilization.
– Amplification of the optical parametric fluorescence (OPF) also called superfluorescence Kleinman (1968), which generates an incoherent background like ASE in lasers and increases with the gain and pump intensity.
– Carrier envelope phase stabilization Baltuska et al. (2003) of the few-cycle pulses turns into an inevitable though challenging task.

As discussed above the finite pump pulse duration corresponds to a finite temporal gain window. Outside of this window the undesired background like ASE, OPF or prepulses is not amplified and so the contrast gets better outside by a factor of the parametric gain. Presently OPCPA with short pump pulses -in the ps range- is mainly used for the generation of few-cycle pulses Herrmann et al. (2009); Gu et al. (2009); Major et al. (2009), that are unachievable with other methods. The good contrast is a extra benefit from OPCPA and can be well utilized only in ultra-high intensity few-cycle systems.

2.2.2 Plasma mirror

Intense focused laser pulse impinging onto a transparent target for the laser wavelength -typically glass- start to generate plasma when the intensity exceeds the damage threshold of the material. The target is ionized and an expanding plasma is generated on the surface with an expansion velocity about the plasma sound speed (0.1 nm/fs at 1 keV plasma temperature). A high density plasma layer is formed and as soon as the electron density in the plasma exceeds the critical density for the incident wavelength as defined by Eq. 1 its reflectivity for the incident pulse switches to a high value. The remaining part of the laser pulse and everything afterward are reflected. The low intensity prepulses and the pedestal are transmitted through the transparent substrate before the plasma formation. This way, a

low reflectivity is used for the prepulses and the pedestal, while a several orders of magnitude higher reflectivity value is applied for the main pulse. This fast plasma shutter is well suited for suppression of unwanted light before the main pulse. Consequently the contrast of the pulse is increased by the ratio of the plasma reflectivity to cold or Fresnel surface reflectivity of the material. The contrast improvement is typically 2 to 3 orders of magnitude with AR coated targets and *s* incident polarization or in a geometry with an incidence angle close to Brewster's angle and *p*-polarization. If the plasma scale length -see Eq. 2- exceeds the laser wavelength the plasma starts to absorb and distort the phasefront of the reflected pulse leading to lower reflectivity and the loss of beamed specular reflection Hörlein et al. (2008). The principle of the plasma mirror is illustrated in Fig. 4.

The plasma mirror Kapteyn et al. (1991) is used to improve the laser pulse after amplification and compression and provides higher throughput without limitation on the input energy Gibbon (2007). Since it is used after the whole laser system, the plasma mirror can be implemented without any modification to the system itself. Further advantages are wide bandwidth acceptance as will be discussed later Nomura et al. (2007), and spatial filtering effect if the plasma mirror is in the vicinity of the laser focus Gold (1994); Doumy et al. (2004a); Hörlein et al. (2008), but no smoother beam profile or even degradation was reported using the target in the near-field Dromey et al. (2004); Hörlein et al. (2008). Several investigations in different geometries Backus et al. (1993); Ziener et al. (2002); Doumy et al. (2004a) as normal, 45° and Brewster's angle of incidence were conducted to study the reflectivity of the plasma mirror yielding 50-80% overall -time- and space-integrated- energy reflectivity and a measured contrast enhancement of 50-100 for *s*-polarization and antireflection coated targets Dromey et al. (2004); Monot et al. (2004) and 25-50% energy throughput and 50-400 enhancement for *p*-polarization and Brewster's angle Backus et al. (1993); Nomura et al. (2007). The temporally resolved reflectivity during the plasma mirror is formed was measured to be 300-1000 fs determined with 100-500 fs laser pulses Bor et al. (1995); von der Linde et al. (1997); Grimes et al. (1999). Some studies pursued the application possibility of the plasma mirror: improving the repetition rate by using a liquid jet as the target Backus et al. (1993) and

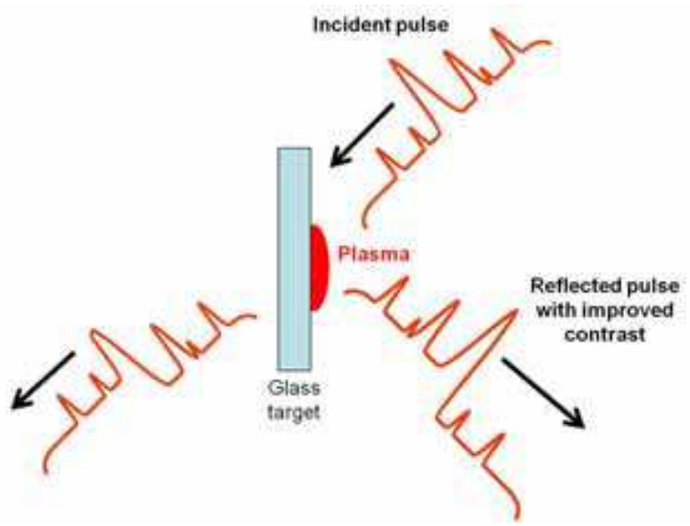

Fig. 4. Working principle of the plasma mirror. The incident low intensity prepulses and pedestal are transmitted through the transparent glass target, while the foot of the high intensity main pulse generates a plasma, which reflects the main pulse.

cascading two plasma mirrors with an overall reflectivity of 31-50% to improve the contrast by $10^4 - 5 \times 10^4$ to reach a required level in the experiments Wittmann et al. (2006); Lévy et al. (2007); Thaury et al. (2007); Doumy et al. (2004b). All previous studies used pulses with 25 fs of duration or longer and only our investigations Nomura et al. (2007) and others shown later applied sub-10-fs pulses. On the other hand, intense few-cycle pulses with a sufficiently high contrast would open up a new prospect for many applications as intense single attosecond pulse generation Tsakiris et al. (2006). Therefore it has great significance to study the possibility to obtain high-contrast few-cycle pulses using a plasma mirror.

2.2.3 Cross-polarized wave generation

Light propagating in nonlinear optical crystals experiences the partial conversion into light with perpendicular polarization. This additional component is called the cross-polarized wave (XPW) Minkovski et al. (2004; 2002). There are two different processes leading to XPW generation: the nonlinear polarization rotation -an elliptic polarization state remains elliptic with the same ellipticity just the main elliptical axis is rotated- and the induced ellipticity -the ellipticity changes, but the main elliptical axis stays the same. XPW generation is a third order nonlinear effect originating in practice from the dominant real part of $\chi^{(3)}$. The XPW efficiency is proportional to the product of $\chi^{(3)}_{xxxx}$ and the anisotropy of the $\chi^{(3)}$ tensor Minkovski et al. (2004). It has perfect and simultaneous phase- and group-velocity matching due to the same frequencies of input and output beams and propagation along the optical axis, which results in high efficiencies. Typically BaF_2 or LiF is used in the experiments since it has moderate $\chi^{(3)}_{xxxx}$ and high anisotropy leading to high-efficiency XPW generation ($\geq 10\%$) without significant self-phase modulation, which depends only on $\chi^{(3)}_{xxxx}$. The XPW process was applied to femtosecond pulse cleaning as the temporal third order nonlinearity suppresses low intensity light surrounding the main laser pulse. Typical schematics of the XPW setup is shown in Fig. 5. The polarization of the beam input with an energy from a few μJ to a few mJ is cleaned by a polarizer and it is focused to reach the required $3 - 7 \times 10^{12}$ W/cm^2 intensity in the BaF_2 crystal, which is typically not in the focus. Here the orthogonally polarized component is generated with 10% efficiency if the angle β between the laser polarization and the x axis of BaF_2 is optimized, which for [001] or z-cut crystals weakly depends on the intensity for high intensities. Subsequently the beam is collimated and send through an analyzer to remove the original polarization. The contrast after the filter neglecting saturation Jullien et al. (2006b):

$$C_{out} = C_{in}^3 + C_{in} K R / \eta_{eff}, \tag{3}$$

where $C_{in/out}$ is the contrast at the input/output of the contrast filter ($C_{in} = 10^{-2} - 10^{-8}$), R is the polarizer extinction ratio ($R = 10^{-2} - 10^{-5}$), η_{eff} is the internal energy efficiency ($\eta_{eff} = 0.1 - 0.2$) and $K = \eta_{eff}/\eta_{peak} \sim 0.2$ is an integration constant connecting the effective efficiency and the peak efficiency (η_{peak}) and originating from temporal and spatial profiles. This equation indicates that the output contrast is proportional to the third power of the input contrast, but the improvement is limited by the polarizer extinction ratio. Therefore high quality polarizers with low extinction ratios and good input contrast provides a better enhancement. This might be slightly influenced by saturation very near to the pulse peak.
The XPW leads to 3-5 OOM enhancement and 10-11 OOM laser contrast Jullien et al. (2005); Chvykov et al. (2006). A double crystal scheme was also applied to increase the efficiency to 20-30% due to the nonlinear self focusing that increases the intensity in the second crystal, the different corresponding Gouy phase shift between fundamental and XPW providing an

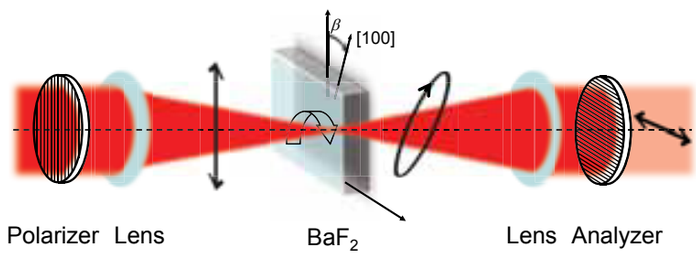

Fig. 5. Schematics of cross-polarized wave generation

optimal phase difference at the second crystal and the possibility of independent optimization of β Chvykov et al. (2006); Jullien et al. (2006a;b). BaF_2 with holographic cut orientation [011] further increases the efficiency. 11.4% and 28% were demonstrated in single and double crystal scheme as the coupling coefficient is slightly higher in this case Canova et al. (2008a). Further advantages of the holographic cut is that β is not intensity dependent allowing better phase matching at high intensities. XPW in BaF_2 is suitable for a broad wavelength range from UV to near-IR Canova et al. (2008b); Cotel et al. (2006); Jullien et al. (2006a). A significant smoothing and a $\sqrt{3}$ broadening of the spectrum is generated by the XPW as it is a third order temporal nonlinearity, which was observed experimentally in the case of optimal compression Jullien et al. (2007); Canova et al. (2008c). An even a larger broadening and pulse shortening of a factor of 2.2 was measured with a spatially super-Gaussian beam from a Ti:sapphire laser having 23% -even up to 28%- internal efficiency as a consequence of an interplay between cross- and self-phase modulation of the XPW and fundamental waves and the strong saturation Jullien et al. (2008). XPW with few-cycle pulses was also demonstrated Jullien et al. (2009; 2010), it shows spectral intensity and phase smoothing and preserves the carrier envelope phase Osvay et al. (2009). Up to now only a limited (2 OOM) contrast improvement of XPW with few-cycle pulses was experimentally supported Jullien et al. (2010). Reaching high efficiency needs $\sim$mm crystal thickness which changes significantly the pulse duration of sub-10-fs pulses during propagation in the crystal due to dispersion. Therefore it is not clear whether the XPW technique is applicable to few-cycle pulses and a higher contrast improvement accessible.

2.2.4 Characterization of contrast

Various measurement techniques of laser contrast are discussed in this session. The difficulties in measuring the contrast are the required high dynamic range of higher than 8 OOM and the good temporal resolution approaching the pulse duration of the main pulse. A normal photo diode for example has a dynamic range of 3-4 OOM and a temporal resolution of about 100 ps. None of these properties is suitable for a detailed contrast determination. Principally a simple second harmonic autocorrelation measurement routinely applied for pulse duration measurement delivers already information about the foot of the pulse with 3-4 OOM dynamics Roskos et al. (1987); Antonetti et al. (1997) and under certain conditions this measurement limit can be extended to 7-9 OOM for example using Lock in detection Braun et al. (1995); Curley et al. (1995). The time ambiguity is certainly present in these investigations using the second harmonic and so the leading and trailing edges are not distinguishable. To this end autocorrelation based on the surface-enhanced third harmonic signal with Lock in detection was used with a 1 kHz system providing a dynamics of 10^5 Hentschel et al. (1999). Still the required measurement dynamics is not reached and typical ultrahigh intensity lasers

have low repetition rate ($\sim$10 Hz) prohibiting the use of Lock in detection. Cross correlation based on third harmonic generation (THG) in two subsequent nonlinear crystals provides both high dynamic $>$ 10 OOM and free from time ambiguity Luan et al. (1993); Antonetti et al. (1997); Aoyama et al. (2000); Tavella et al. (2005). Even a single shot version of this cross-correlator was realized for low repetition rate high energy laser systems Dorrer et al. (2008); Ginzburg et al. (2008). Nowadays THG cross-correlation is the most popular method to characterize contrast. An alternative way is the optical parametric amplifier correlator (OPAC) Divall & Ross (2004); Witte et al. (2006), which is based an optical parametric amplification of the fundamental in a short temporal window defined by the frequency doubled pump. The detection limit is 11 OOM with a theoretical value of 15 OOM. Recently specular reflectivity of overdense plasmas applied to estimate the contrast Pirozhkov et al. (2009) giving a measure of the preplasma generated by the general preceding background. An extended preformed plasma leads to beam breakup and increased absorption so a sufficiently good contrast gives a high reflectivity even at ultra-relativistic intensities.
We applied a THG cross-correlator, the upgraded version of that in Ref. Tavella et al. (2005), capable to measure 10-11 OOM to determine the contrast improvement separately by the implemented techniques.

3. Results and discussion

In this chapter various efforts to improve the contrast on two different few-cycle light sources will be discussed. The first system is a Titanium:sapphire laser with 1 kHz repetition rate Verhoef et al. (2006) and the second is an OPCPA system, called Light Wave Synthesizer 20 Herrmann et al. (2009). A plasma mirror was realized and characterized with the first system described in chapter 3.1, while short pump OPCPA was ”implemented” in LWS-20 and XPW and plasma mirror are planned to be implemented in the near future to obtain a unique contrast as discussed in chapter 4.

3.1 Plasma mirror with a kHz Titanium:sapphire laser

A plasma mirror was implemented in a few-cycle laser system and characterized in detail Nomura et al. (2007); Nomura (2008). The reflectivity and the focusability were determined in *s*- and *p*-polarization and the time resolved contrast improvement was also measured. The source was a broadband 1 kHz Ti:sapphire laser system based on chirped pulse amplification with three multi-pass amplifier stages and a hollow-fiber compressor Verhoef et al. (2006). The system typically delivered pulses with 550 μJ energy, a spectrum extending from 550 to 900 nm with a central wavelength of 730 nm and 7 fs duration at 1 kHz repetition rate as shown in Fig. 6. The output beam was guided through a vacuum beamline to the target chamber. The energy on the target was 350-400 μJ.
The experimental setup is shown in Fig. 7. Either *p*- or *s*-polarization of the incident beam could be set by changing the alignment of a periscope before entering into the target chamber. The beam with 50 mm diameter was focused onto a 120 mm diameter BK7 glass target with an f_{eff} = 150 mm, 90$\circ$ silver off-axis paraboloid mirror (F/3) leading to a focus full width at half maximum (FWHM) diameter of 7-8 μm. Three motorized stages allowed to rotate the target and translate it parallel to the surface and parallel to the incident beam (defined as z-direction). At 1 kHz repetition rate a target lasted approximately for an hour. The reflected beam from the target was refocused with a thin achromatic lens and sent to a detector outside the vacuum chamber. We measured the reflected energy using a power meter as detector; the spatial peak reflectivity by imaging the beam profile around the focus of the incident and

the reflected beam with a microscope objective onto a charge-coupled device (CCD) camera; and the temporal structure with high dynamics of the incident and also of the reflected pulses using a third-order correlator.

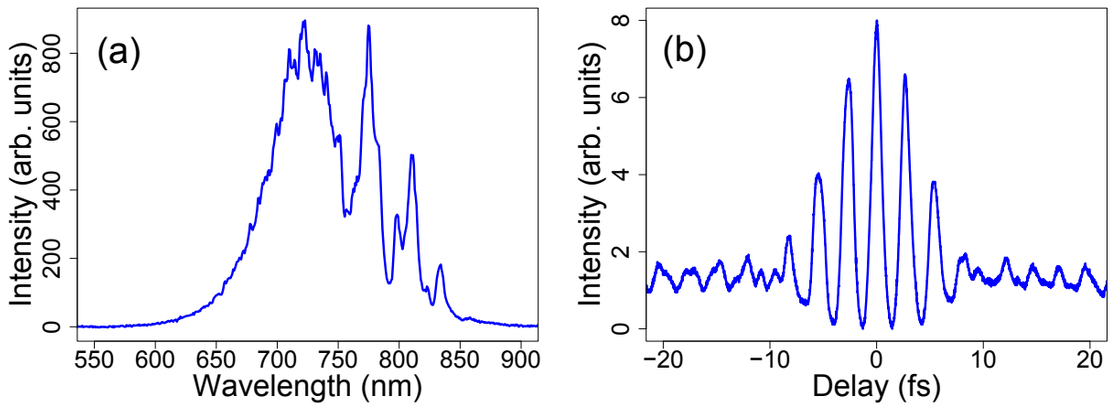

Fig. 6. Typical spectrum (a) and interferometric second-order autocorrelation (b) of the Ti:sapphire laser pulses used in the first plasma mirror experiment. The pulse duration is about 7 fs.

The plasma mirror efficiency was characterized by the energy throughput, i.e. the spatially integrated or average reflectivity, and the peak reflectivity. We calculate the peak reflectivity as the ratio of the peak fluences, which are obtained from the measured beam profiles on the target and energies. As we will see, this gives the same as the ratio of the peak intensities, which is the definition of the reflectivity. The energy measured with the power meter was averaged over some thousand shots. The incident fluence was changed by either moving

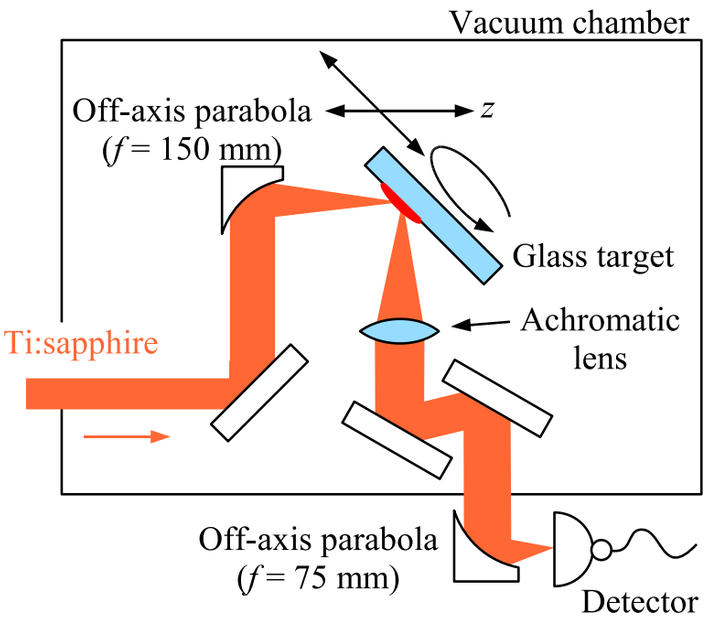

Fig. 7. Experimental setup

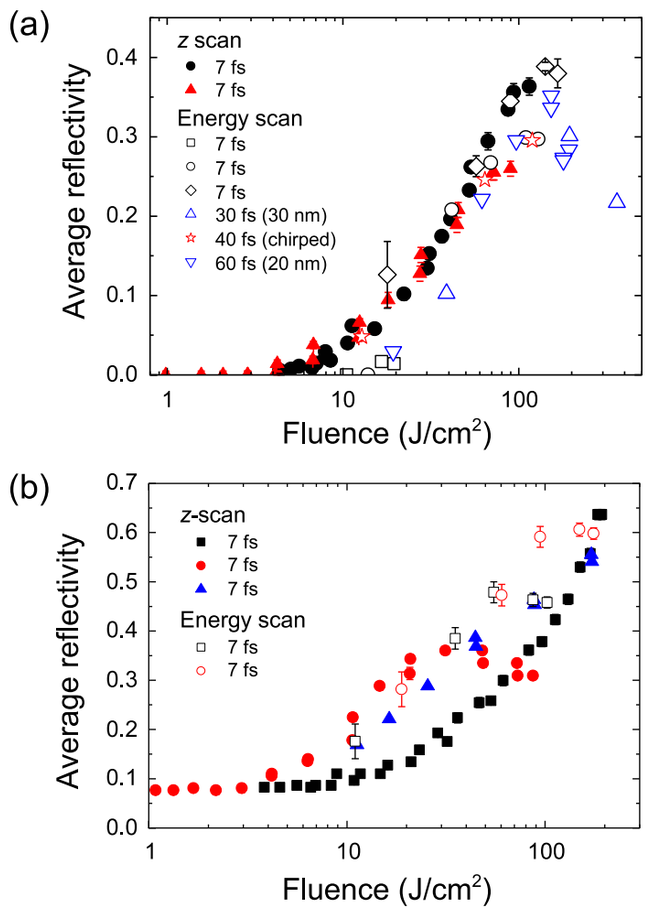

Fig. 8. Average reflectivity of the plasma mirror for (a) *p*-polarization and (b) *s*-polarization as a function of the average incident fluence. Different symbols represent different sets of measurements containing also runs with elongated pulses due to chirp or clipped spectrum. For *p*-polarization, the highest and lowest reflectivity measured are $\sim 40\%$ and $\sim 0.5\%$, respectively, therefore a contrast improvement of two orders of magnitude is expected.

the target out of focus (z-scan) or decreasing the energy of the incident pulse (energy scan). Different sets of measurements are shown with different symbols in Fig. 8. The measurements were well reproducible and gave the same results for z-scan and for energy scan. We also measured the average reflectivity with longer pulse durations, which was achieved by either chirping the pulse or clipping the spectrum. Therefore, we plotted the reflectivity as a function of the incident fluence in Figs. 8, 9.

Fig. 8 (a) shows the average reflectivity for *p*-polarization as a function of the average incident fluence, which is determined with respect to the spatial full width at half maximum (FWHM) area of the focused beam. The highest average reflectivity reached up to $\sim 40\%$ between 100 and 150 J/cm^2, whereas the lowest reflectivity was as low as $\sim 0.5\%$ because the 45° incidence angle was close to Brewster's angle ($\sim 56°$). From these values, a contrast improvement of two orders of magnitude is expected. The pulse duration was increased up to 60 fs, i.e., a factor of 9, but no significant change was observed in the behavior of the reflectivity versus fluence dependence. The average reflectivity measured for *s*-polarization is plotted in

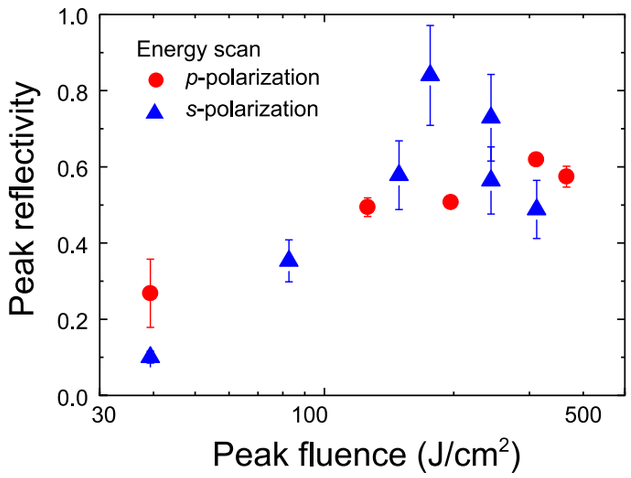

Fig. 9. Spatial peak reflectivity of the plasma mirror for *p*- and *s*-polarization plotted against the spatial peak incident fluence.

Fig. 8 (b). The highest reflectivity reached up to $\sim 65\%$ and might be even higher for higher fluence on target unavailable in this experiment. In spite of the higher average reflectivity, the expected contrast improvement is only one order of magnitude due to the relatively high Fresnel reflectivity at *s*-polarization, which is $\sim 8\%$ at 45° angle of incidence for our target material. The results plotted in Fig. 8 (b) had larger fluctuations than those in Fig. 8 (a) due to the different laser conditions. Reducing the reflectivity with antireflection (AR) coated targets can boost the contrast improvement up to factor of 300 and have maximal throughput. Using *p*-polarized light allows us to use cheaper uncoated glass targets at the cost of decreased throughput ($\sim 40\%$). The contrast improvement factors are in the same order for *s*-polarized light with AR-coated targets and for *p*-polarized light with ordinary targets, at 45° incidence angle. Using Brewster's angle increases the improvement factor for *p*-polarization even more, although the alignment is more sensitive.

The spatial peak reflectivity for *p*- and *s*-polarized pulses is depicted in Fig. 9 as a function of the peak fluence. The maximum value was above 60% for *p* and above 80% for *s* polarization. The spectra of the incident and reflected pulses were also measured, but they were almost identical and no significant blue shift was observed.

It is important for applications of the plasma mirror that the reflected light is still focusable and the wavefront and beam profile are not degraded. To investigate the spatial characteristics of the reflected beam, we collimated it with an achromatic lens (f = 150 mm) and refocused with an f = 75 mm off-axis parabola. The image of the refocused spot was magnified with a microscope objective and captured by a CCD beam profiler. The target was moved in the focal (z) direction and the imaging system was adjusted for each measurement. The measured spot diameters are plotted in Fig. 10 (a). The horizontal lines indicate the spot diameter without activating the plasma mirror, i.e., with low input energy. The different focus diameters for *s*- and *p*-polarizations are due to different alignments of the beamline. A horizontal and a vertical lineout of the refocused beam profile are plotted for *s*-polarization with (solid) and without (dashed) plasma mirror in Fig. 10 (b) when the target was in the focus (z = 0). We observed two effects on the reflected beam: cleaner smoothed near-field beam profile and smaller refocused spot. Both changes can be explained by the fluence-dependent reflectivity of the plasma mirror. The plasma mirror reflects more efficiently at the central part of the beam, while the reflection at the surrounding area is relatively suppressed, which acts as

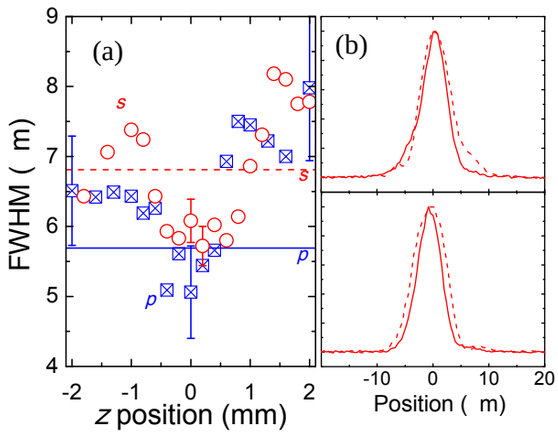

Fig. 10. (a) Refocused spot size (FWHM) as a function of the plasma-mirror position in the focal (z) direction. The polarization of the incident beam was *p* (blue square) or *s* (red circle). Horizontal lines indicate the reference spot size without activating the plasma mirror for *p* (solid) and *s* (dashed) polarization. (b) Horizontal and vertical lineouts of the refocused beam profile with the target in the focus (z = 0) for *s*-polarization with (solid) and without (dashed) plasma mirror.

a spatial filter resulting in a cleaner beam profile Moncur (1977). At the same time, this fluence-dependent reflectivity makes the peak narrower, which results in a smaller spot size on the plasma mirror and consequently a smaller refocused spot size.

The most important property of a plasma mirror is the contrast enhancement factor that is estimated based on cold and hot plasma reflectivity in general, but it is rarely verified experimentally. We present a complete high-dynamic-range third-order correlation of the reflected pulses, which allows us to obtain the time-resolved reflectivity and contrast enhancement of the plasma mirror. The polarization of the beam incident to the target was set to *p* to realize a better contrast improvement. The fluence on the plasma mirror was estimated to be ~ 60 J/cm^2 corresponding to about 30% average reflectivity. The reflected beam was recollimated and sent into a home-made third-order correlator Tavella et al. (2005). Fig. 11 shows the measured third-order correlation of the reflected pulse together with that of the incident pulse. The negative delay represents the leading edge of the pulse as before. Although the measured contrast was limited by the low energy of about 50 μJ sent into the correlator, the expected contrast improvement of two orders of magnitude at the pulse front is striking, for example, around -2 or at -8.5 ps. The peak appearing at -1.5 ps is an artefact from a post pulse, which appears due to the nature of correlation measurements. Also a pulse steepening effect is evident on the rising edge. On the other hand, no effect is observed on the falling edge of the pulse. Since 100 μm thick crystals were used in the correlator to gain a stronger signal, the third-order correlation does not reflect the short pulse duration.

Fig. 12 depicts the time-resolved reflectivity of the plasma mirror for *p*-polarization obtained by dividing the correlation of the reflected pulse by that of the incident pulse. We normalized the curve by setting the average reflectivity between 0 and 4 ps to the expected peak reflectivity of 50%.

A steep rise in the reflectivity is clearly seen at -500 fs. This steep rise indicates that the plasma is generated 400-500 fs before the main pulse. Therefore, the plasma mirror is efficiently

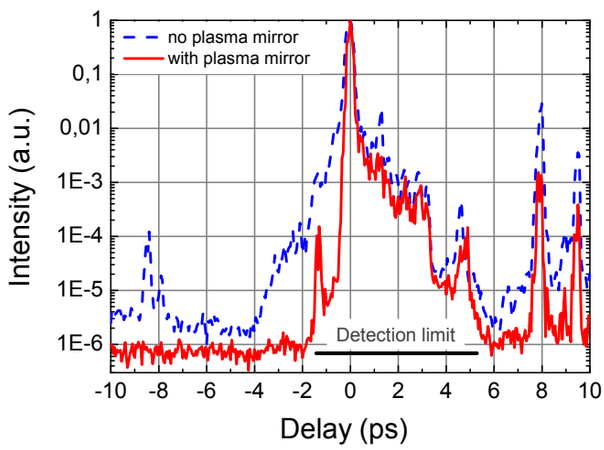

Fig. 11. Measured contrast without (black) and with (red) the plasma mirror using *p*-polarization. Although the measured contrast was limited by the low input energy ($\sim 50\mu$J), contrast improvement of two orders of magnitude is seen in the leading edge, for example, around -2 ps.

generated with the pedestal of our sub-10-fs pulses, similarly to the previous experiments with longer pulses. It is apparent that the reflectivity is constant during the pulse, hence the way we attained the peak reflectivity using the fluences is correct.A decrease in the reflectivity is also visible ~ 6 ps after the main pulse.
Hydrodynamic simulation of the preformed plasma expansion with a simulation code MEDUSA Christiansen et al. (1974) was performed to further understand the physical process. The input pulse used for the simulation was a 7 fs Gaussian pulse sitting on a 1.7 ps Gaussian

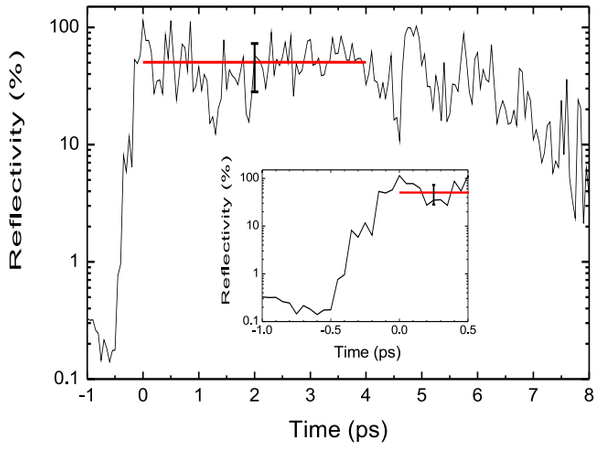

Fig. 12. Time-resolved peak reflectivity of the plasma mirror calculated from the correlations in Fig. 11. The horizontal red line is the average value of the peak reflectivity between 0 and 4 ps and the error bar corresponds to the standard deviation. Inset: the fast increase of the reflectivity at the leading edge.

pedestal with 2×10^{-4} contrast and a 7 fs Gaussian prepulse 8.5 ps before the main peak with 10^{-4} contrast as shown in Fig. 13. These parameters were determined by fitting the third-order correlation trace measured without the plasma mirror. The result of the simulation is also shown in Fig. 13. The simulation shows that the scale length of the plasma (Eq. 2) is $\sim 0.03\lambda$ at the critical density (Eq. 1) when the peak of the pulse arrives. If the scale length is too large, a plasma mirror acts similarly to a chirped mirror because different wavelengths are reflected at different depths in the plasma surface, owing to the different critical densities. With this scale length, however, this chirping effect is negligible and the pulse duration stays the same after the plasma mirror. The simulation also shows that the scale length exceeds 0.1λ around +2 ps after the main peak. Above this scale length, the process of resonant absorption starts Gibbon & Bell (1992), and reaches its maximum efficiency around $L = 0.3\lambda$ Kruer (1988). The simulation shows that this scale length is reached around +4 ps, which explains the decrease of the reflectivity around 6 ps.
In spite of the detailed measurements the preservation of the few-cycle pulse duration by the plasma mirror was just indirectly supported. In chapter 4 this important property will also be further discussed.

3.2 Contrast improvement of an OPCPA system

The second few-cycle light source, in which we applied contrast enhancement is the 8-fs, 16-TW OPCPA system, Light Wave Synthesizer 20 (LWS-20) Herrmann et al. (2009). This chapter describes the results from the short pump pulse OPCPA. Later in the next chapter we will discuss the potential if XPW and plasma mirror are also implemented. LWS-20 is the first optical parametric chirped pulse amplifier (OPCPA) system with few-cycle pulse duration and $\sim$20 TW peak power. OPCPA generally offers a unique alternative to conventional lasers with much broader amplification bandwidth and correspondingly much shorter pulses reaching the sub-10-fs range, much higher gain, and low thermal load as analyzed before. In our OPCPA system as shown in Fig. 14 pulses from an ultra-broadband oscillator (Rainbow, Femtolasers), producing $\sim$5.5 fs pulses with 80 MHz repetition rate, are split for optical synchronization. One part is wavelength shifted to 1064 nm to seed a commercial pump

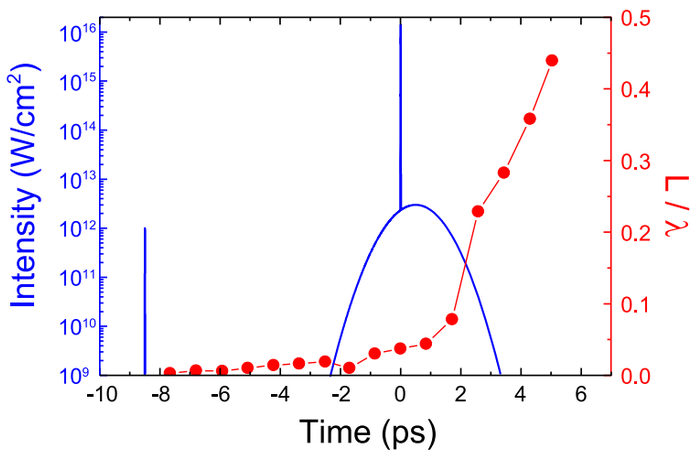

Fig. 13. Evolution of plasma scale length calculated with MEDUSA. Temporal profile of the input pulse (blue curve) estimated from the measurement. Evolution of the plasma scale length (red circles). It stays almost unchanged as the main pulse arrives and starts to increase after most of the pedestal has passed.

laser (EKSPLA) producing up to 1 J, 75 ps, 10 Hz pulses at 532 nm. The main part of the oscillator energy is amplified in a Femtopower Compact Pro 1 kHz Ti:sapphire CPA laser, which tightens the bandwidth and produces 25 fs long pulses after compression in the prism compressor.

These pulses with 750-800 μJ energy are sent into a neon filled tapered-hollow-core fiber to broaden the spectrum to seed the amplifier stages. After an optional XPW stage for contrast enhancement the pulses are stretched to 45 ps -group delay between blue and red spectral components- with a specially designed negative dispersion grism stretcher. An acousto optic programmable dispersive filter (Dazzler, Fastlight) serves the purpose of optimizing and fine tuning the spectral phase. The slightly compressed pulses -to about 30 ps after the Dazzler- are amplified in two non-collinear optical parametric chirped pulse amplifier stages based on type I BBO nonlinear optical crystals. The first stage is pumped by 15 mJ and amplifies the few-μJ seed pulses to about 1 mJ and the second stage is pumped with an energy of up to 800 mJ and delivers up to 170 mJ. The supported wavelength range of the OPA is from 700 nm up to 1050 nm, but due to practical limitations in the Dazzler, only spectral components up to about 980 nm can be used for compression, which corresponds to a Fourier limited pulse duration of 8 fs. The pulses are compressed in a high transmission compressor containing bulk glasses of 160 mm SF57 and 100 mm quartz and by four chirped mirrors to approx. 8 fs. After the compressor a pulse energy of up to 130 mJ is reached with 10 Hz repetition rate. A Shack-Hartmann wavefront sensor (Imagine Optic) and an adaptive mirror in a closed loop configuration are used to optimize the wavefront and so the focusing properties of the laser to reach $\gg 10^{18}$ W/cm^2 relativistic intensity on target. The system is ideally suited for electron acceleration in the non-linear laser wakefield acceleration regime with high efficiency and

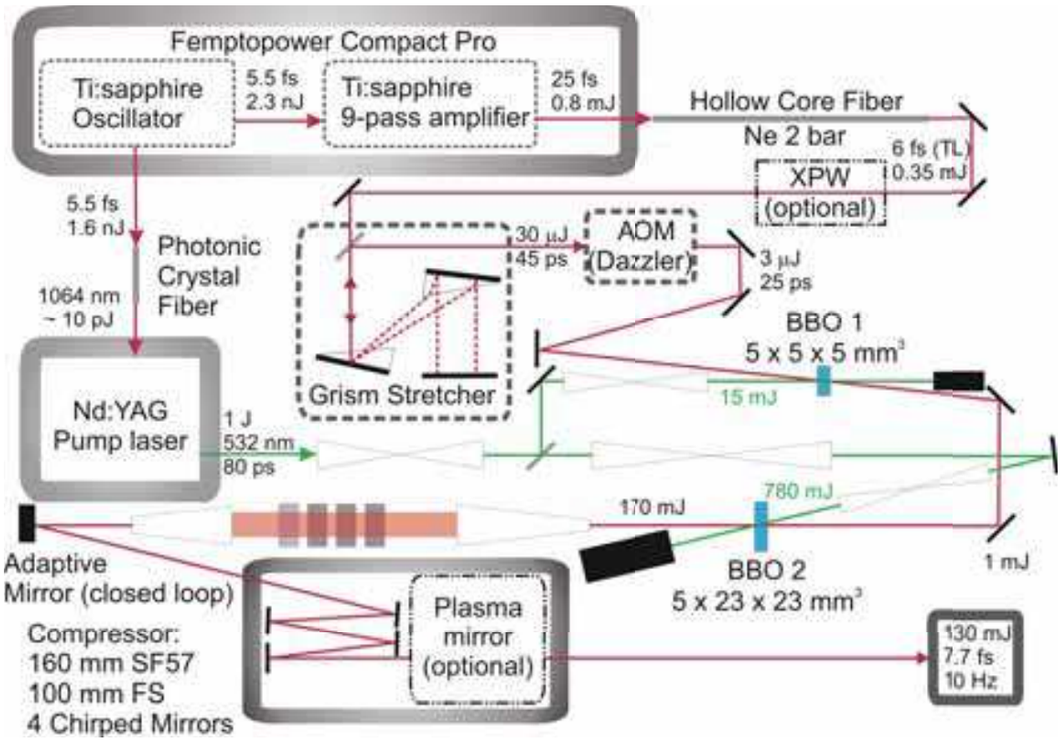

Fig. 14. Setup of the Light Wave Synthesizer 20 (LWS-20) OPCPA system.

stability to generate monoenergetic electrons Schmid et al. (2009) as well as for high harmonic generation towards a single attosecond pulse generation on plasma surfaces Heissler et al. (2010) and gas jets. Carrier envelope phase (CEP) measurements are also envisaged for CEP stabilization that will be necessary to generate single attosecond bursts.
As discussed before the contrast is improved in a short pulse (75 ps in our case) OPCPA system outside the pump duration. In LWS-20 the input contrast from the kHz front end is between 7-8 orders of magnitude (OOM) and it is conserved in approx. $\pm$40 ps temporal window and many orders of magnitude better outside this window as shown in Fig. 15 blue dashed line. There is a 5 ps pedestal originating from stretching and compression. This is suppressed to 10^{-8} in the best case without other contrast enhancement as will be discussed later. The background from -5 ps up to -20 ps is the ASE from the front end amplified in the OPCPA stages. After the main pulse a longer continuously decreasing pedestal coming from the hollow-core fiber follows. The expected contrast enhancement $>$ 40 ps before the pulse peak is 10^5 as the amplification increases the energy from about 1 μJ to on the order of 100 mJ. Although the third order correlator is capable of measuring 10 OOM it is still not enough to correctly determine the improvement in the contrast outside the pump temporal extension. Therefore we misaligned the front end -attenuated the multipass seed- to reduce the ASE contrast to deliver 5-6 OOM contrast. This reduced contrast is preserved in the OPCPA chain (at -6 ps 10^{-5}), but suppressed before the pump (at -45 ps 10^{-10}) as indicated by the red curve in Fig. 15. As a conclusion the OPCPA with short pump pulses improves the contrast corresponding to the gain coefficient by 5 OOM.

4. Conclusion and future work

In conclusion, the contrast improvement of sub-10-fs pulses by using a plasma mirror and OPCPA are demonstrated. The reflected pulses from the plasma mirror were cleaned both spatially and temporally. The spatial peak reflectivity reached $\geq$ 80% ($\geq$ 60%) and the energy

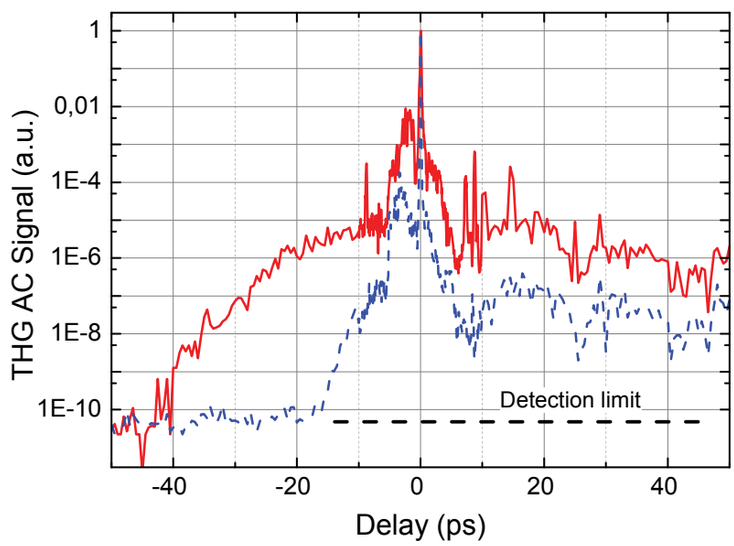

Fig. 15. Contrast of the LWS-20 OPCPA system (blue dashed line) and contrast with misaligned frond end to visualize the 10^5 enhancement between -6 and -45 ps due to OPCPA (red solid line).

throughput had a value of $\sim$ 65% ($\sim$ 40%) for *s*- (*p*-) polarization at 45° angle of incidence. Using AR coated targets and *s*-polarization an average reflectivity of 70-80% is expected. The first measurement of the complete high-dynamic-range correlation revealed the temporal structure of the pulses reflected from the plasma mirror. The time-resolved reflectivity of the plasma mirror was determined with the help of these results, showing the contrast improvement of two orders of magnitude and the pulse steepening at the leading edge. This enhancement can be further increased to min. 2.5 orders of magnitude with AR coated targets. Improving the contrast with the plasma mirror will lead to better performances in experiments such as high-order harmonic generation on plasma surfaces or ion acceleration. The plasma mirror reflectivity is found to be independent on the chirp of the the incident pulses, which allows to optimize the pulse duration on a second target. The pulse spectrum was practically the same before and after the plasma mirror. Therefore the fact whether the plasma mirror pertains the short duration is not significant. On the other hand, the final size of the plasma mirror target will impose a limit on the number of laser shots in one experimental run. The use of the plasma mirror should be determined by weighing the benefits gained by the contrast improvements against the drawback of the limited number of shots. In the case of a moderate energy system ($\sim$ 100 mJ) many hours operation with 10 Hz repetition rate is principally possible.

The OPCPA technique with short pump pulses has among others also a big advantage in background suppression. Using moderate saturation a contrast improvement corresponding to the gain is achievable outside of the pump pulse duration. In our OPCPA system, LWS-20, an enhancement of 10^5 is realized with 80 ps pump pulses. Using even shorter pump lasers ($\sim$ 1 ps) this window is significantly reduced, but other difficulties as pump seed synchronization or non-linear effects in air and other optical components may arise. Hybrid laser systems utilize this advantage and the final high-energy laser amplification, which is presently a challenge for the short pulse pump laser. Comparing the plasma mirror to the OPCPA technique both of them have advantages and draw backs. The OPCPA amplifies already with an improved contrast, but only outside the pump window is the contrast better while the plasma mirror enhances the contrast also directly before the pulse peak, steepens the rising edge and removes background generated after the front end very near to the main pulse. The XPW technique is robust and has a large improvement, but enhances the input contrast into the amplifier and removes background just from the front end and cannot affect reasons for worse contrast that are generated later. The decision which of the methods is best suited in a given system is not easy to answer and can depend from case to case.

To further improve the contrast for experiments with LWS-20 a cross-polarized wave (XPW) generation cleaner stage (see Chapter) and a plasma mirror are planned to be implemented. The structure of LWS-20 is ideally suited to implement XPW after the hollow-core fiber and before the grism stretcher. This structure makes it practically to a double-CPA system Kalashnikov et al. (2005) with an OPCPA instead of CPA as the second amplification part. The expected contrast improvement using Eq. 3 and a Glan-Laser polarizer with an extinction ration of better than $2 - 5 \times 10^{-4}$ is up to 10^{-4}. The plasma mirror with AR coated targets having 0.2% reflectivity and an estimated plasma mirror reflectivity of 60% is expected to enhance a contrast by about 3×10^{-3} and also steepen the rising edge if the pulses. After the implementation of XPW about 10^{-17} and the implementation of the plasma mirror about 10^{-19} contrast is expected 45 ps before the pulse peak. These values and the good contrast also before this delay makes the LWS-20 system an ideal candidate as a front end of future multi-Petawatt to Exawatt lasers.

5. Acknowledgments

The author gratefully acknowledge the work on the laser system in Vienna of A. J. Verhoef, J. Seres, E. Seres, G. Tempea and the work done on the plasma mirror by J. Nomura, K. Schmid, T. Wittmann and J. Wild. Furthermore the work on LWS-20 or its predecessors by D. Herrmann, R. Tautz, F. Tavella, A. Marcinkevičius, V. Pervak, N. Ishii, A. Baltuška is acknowledged as well as the users who contributed to the system significantly as A. Buck, J. M. Mikhailova, K. Schmid, C. M. S. Sears, Y. Nomura. Furthermore grateful thanks are due to G. Tsakiris. Extra thanks to Prof. F. Krausz for his support. A. Buck, J. M. Mikhailova, T. Wittmann are acknowledged for reading and correcting the manuscript.

6. References

Antonetti, A., Blasco, F., Chambaret, J. P., Cheriaux, G., Darpentigny, G., Le Blanc, C., Rousseau, P., Ranc, S., Rey, G. & Salin, F. (1997). A laser system producing 5×10^{19} w/cm^2 at 10 hz, *Appl. Phys. B* 65: 197–204.

Aoyama, M., Sagisaka, A., Matsuoka, S., Akahane, Y., Nakano, F. & Yamakawa, K. (2000). Contrast and phase characterization of a high-peak-power 20-fs laser pulse, *Appl. Phys. B* 70: S149–S153.

Backus, S., Kapteyn, H. C., Murnane, M. M., Gold, D. M., Nathel, H. & White, W. (1993). Prepulse suppression for high-energy ultrashort pulses using self-induced plasma shuttering from a fluid target, *Opt. Lett.* 18(2): 134.

Baltuska, A., Udem, T., Uiberacker, M., Hentschel, M., Goulielmakis, E., Gohle, C., Holzwarth, R., Yakovlev, V. S., Scrinzi, A., Hansch, T. W. & Krausz, F. (2003). Attosecond control of electronic processes by intense light fields, *Nature* 421(7075): 611–615.

Bor, Z., Racz, B., Szabo, G., Xenakis, D., Kalpouzos, C. & Fotakis, C. (1995). Femtosecond transient reflection from polymer surfaces during femtosecond uv photoablation, *Appl. Phys. A* 60: 365–368.

Brabec, T. & Krausz, F. (2000). Intense few-cycle laser fields: Frontiers of nonlinear optics, *Rev. Mod. Phys.* 72(2): 545–591.

Braun, A., Rudd, J. V., Cheng, H., Mourou, G., Kopf, D., Jung, I. D., Weingarten, K. J. & Keller, U. (1995). Characterization of short-pulse oscillators by means of a high-dynamic-range autocorrelation measurement, *Opt. Lett.* 20(18): 1889–1891.

Canova, L., Albert, O., Forget, N., Mercier, B., Kourtev, S., Minkovski, N., Saltiel, S. & LopezMartens, R. (2008c). Influence of spectral phase on cross-polarized wave generation with short femtosecond pulses, *Appl. Phys. B* 93: 443–453.

Canova, L., Kourtev, S., Minkovski, N., Jullien, A., Lopez-Martens, R., Albert, O. & Saltiel, S. M. (2008a). Efficient generation of cross-polarized femtosecond pulses in cubic crystals with holographic cut orientation, *Appl. Phys. Lett.* 92(23): 231102.

Canova, L., Kourtev, S., Minkovski, N., Lopez-Martens, R., Albert, O. & Saltiel, S. M. (2008b). Cross-polarized wave generation in the uv region, *Opt. Lett.* 33(20): 2299–2301.

Cerullo, G. & De Silvestri, S. (2003). Ultrafast optical parametric amplifiers, *Rev. Sci. Instrum.* 74(1): 1–18.

Christiansen, J. P., Ashby, D. E. T. F. & Roberts, K. V. (1974). MEDUSA a one-dimensional laser fusion code, *Comput. Phys. Commun.* 7(5): 271–287.

Chvykov, V., Rousseau, P., Reed, S., Kalinchenko, G. & Yanovsky, V. (2006). Generation of 10^{11} contrast 50 TW laser pulses, *Opt. Lett.* 31(10): 1456–1458.

Cotel, A., Jullien, A., Forget, N., Albert, O., Chriaux, G. & Le Blanc, C. (2006). Nonlinear

temporal pulse cleaning of a 1-m optical parametric chirped-pulse amplification system, *Appl. Phys. B* 83: 7–10.

Curley, P. F., Darpentigny, G., Cheriaux, G., Chambaret, J.-P. & Antonetti, A. (1995). High dynamic range autocorrelation studies of a femtosecond ti:sapphire oscillator and its relevance to the optimisation of chirped pulse amplification systems, *Opt. Commun.* 120(1-2): 71 – 77.

Divall, E. J. & Ross, I. N. (2004). High dynamic range contrast measurements by use of an optical parametricamplifier correlator, *Opt. Lett.* 29(19): 2273–2275.

Dorrer, C., Begishev, I. A., Okishev, A. V. & Zuegel, J. D. (2007). High-contrast optical-parametric amplifier as a front end of high-power laser systems, *Opt. Lett.* 32(15): 2143–2145.

Dorrer, C., Bromage, J. & Zuegel, J. D. (2008). High-dynamic-range single-shot cross-correlator based on an optical pulse replicator, *Opt. Express* 16(18): 13534–13544.

Doumy, G., Dobosz, S., D'Oliveira, P., Monot, P., Perdrix, M., Quéré, F., Réau, F., Martin, P., Audebert, P., Gauthier, J. C. & Geindre, J. P. (2004b). High order harmonic generation by non-linear reflection of a pedestal-free intense laser pulse on a plasma, *Appl. Phys. B* 78: 901–904.

Doumy, G., Quéré, F., Gobert, O., Perdrix, M., Martin, P., Audebert, P., Gauthier, J. C., Geindre, J.-P. & Wittmann, T. (2004a). Complete characterization of a plasma mirror for the production of high-contrast ultraintense laser pulses, *Phys. Rev. E* 69(2): 026402.

Dromey, B., Kar, S., Zepf, M. & Foster, P. (2004). The plasma mirror—a subpicosecond optical switch for ultrahigh power lasers, *Rev. Sci. Instrum.* 75: 645.

Dubietis, A., Butkus, R. & Piskarskas, A. P. (2006). Trends in chirped pulse optical parametric amplification, *IEEE J. Sel. Topics Quantum Electron.* 12(2): 163–172.

Dubietis, A., Jonusauskas, G. & Piskarskas, A. (1992). Powerful femtosecond pulse generation by chirped and stretched pulse parametric amplification in bbo crystal, *Opt. Commun.* 88(4-6): 437–440.

Gaul, E. W., Martinez, M., Blakeney, J., Jochmann, A., Ringuette, M., Hammond, D., Borger, T., Escamilla, R., Douglas, S., Henderson, W., Dyer, G., Erlandson, A., Cross, R., Caird, J., Ebbers, C. & Ditmire, T. (2010). Demonstration of a 1.1 petawatt laser based on a hybrid optical parametric chirped pulse amplification/mixed nd:glass amplifier, *Appl. Opt.* 49(9): 1676–1681.

Gibbon, P. (2007). Plasma physics: Cleaner petawatts with plasma optics, *Nature Phys.* 3: 369 – 370.

Gibbon, P. & Bell, A. R. (1992). Collisionless absorption in sharp-edged plasmas, *Phys. Rev. Lett.* 68(10): 1535–1538.

Ginzburg, V. N., Didenko, N. V., Konyashchenko, A. V., Lozhkarev, V. V., Luchinin, G. A., Lutsenko, A. P., Mironov, S. Y., Khazanov, E. A. & Yakovlev, I. V. (2008). Third-order correlator for measuring the time profile of petawatt laser pulses, *Quantum Electron.* 38(11): 1027–1032.

Gold, D. M. (1994). Direct measurement of prepulse suppression by use of a plasma shutter, *Opt. Lett.* 19(23): 2006–2008.

Grimes, M. K., Rundquist, A. R., Lee, Y.-S. & Downer, M. C. (1999). Experimental identification of "vacuum heating" at femtosecond-laser-irradiated metal surfaces, *Phys. Rev. Lett.* 82(20): 4010–4013.

Gu, X., Marcus, G., Deng, Y., Metzger, T., Teisset, C., Ishii, N., Fuji, T., Baltuška, A., Butkus, R., Pervak, V., Ishizuki, H., Taira, T., Kobayashi, T., Kienberger, R. & Krausz, R. (2009).

Generation of carrier-envelope-phase-stable 2-cycle 740-μj pulses at 2.1-μm carrier wavelength, *Opt. Express* 17(1): 62–69.

Hegelich, B. M., Albright, B. J., Cobble, J., Flippo, K., Letzring, S., Paffett, M., Ruhl, H., Schreiber, J., Schulze, R. K. & Fernández, J. C. (2006). Laser acceleration of quasi-monoenergetic MeV ion beams, *Nature* 439(7075): 441–4.

Heissler, P., Hörlein, R., Stafe, M., Mikhailova, J. M., Nomura, Y., Herrmann, D., Tautz, R., Rykovanov, S. G., Földes, I. B., Varjú, K., Tavella, F., Marcinkevičius, A., Krausz, F., Veisz, L. & Tsakiris, G. D. (2010). Towards single attosecond pulses using harmonic emission from solid density plasmas, *Appl. Phys. B* p. accepted.

Hentschel, M., Uemura, S., Cheng, Z., Sartania, S., Tempea, G., Spielmann, Ch. & Krausz, F. (1999). High-dynamic-range pulse-front steepening of amplified femtosecond pulses by third-order dispersion, *Appl. Phys. B* 68(1): 145–148.

Hernandez-Gomez, C., Blake, S. P., Chekhlov, O., Clarke, R. J., Dunne, A. M., Galimberti, M., Hancock, S., Heathcote, R., Holligan, P., Lyachev, A., Matousek, P., Musgrave, I. O., Neely, D., Norreys, P. A., Ross, I., Tang, Y., Winstone, T. B., Wyborn, B. E. & Collier, J. (2010). The vulcan 10 pw project, *J. Phys.: Conf. Ser.* 244(3): 032006.

Herrmann, D., Veisz, L., Tautz, R., Tavella, F., Schmid, K., Pervak, V. & Krausz, F. (2009). Generation of sub-three-cycle, 16 tw light pulses by using noncollinear optical parametric chirped-pulse amplification, *Opt. Lett.* 34(16): 2459–2461.

Homoelle, D., Gaeta, A. L., Yanovsky, V. & Mourou, G. (2002). Pulse contrast enhancement of high-energy pulses by use of a gas-filled hollow waveguide, *Opt. Lett.* 27(18): 1646–1648.

Hörlein, R., Dromey, B., Adams, D., Nomura, Y., Kar, S., Markey, K., Foster, P., Neely, D., Krausz, F., Tsakiris, G. D. & Zepf, M. (2008). High contrast plasma mirror: spatial filtering and second harmonic generation at 10^{19} w/cm^{-2}, *New J. Phys.* 10(8): 083002.

Itatani, J., Faure, J., Nantel, M., Mourou, G. & Watanabe, S. (1998). Suppression of the amplified spontaneous emission in chirped-pulse-amplification lasers by clean high-energy seed-pulse injection, *Opt. Commun.* 148: 70–74.

Jullien, A., Albert, O., Burgy, F., Hamoniaux, G., Rousseau, J.-P., Chambaret, J.-P., Augé-Rochereau, F., Chériaux, G., Etchepare, J., Minkovski, N. & Saltiel, S. M. (2005). 10^{-10} temporal contrast for femtosecond ultraintense lasers by cross-polarized wave generation, *Opt. Lett.* 30(8): 920–922.

Jullien, A., Albert, O., Chériaux, G., Etchepare, J., Kourtev, S., Minkovski, N. & Saltiel, S. M. (2006a). A two crystal arrangement to fight efficiency saturation in cross-polarized wave generation, *Opt. Express* 14(7): 2760–2769.

Jullien, A., Augé-Rochereau, F., Chériaux, G., Chambaret, J.-P., d'Oliveira, P., Auguste, T. & Falcoz, F. (2004). High-efficiency, simple setup for pulse cleaning at the millijoule level by nonlinear induced birefringence, *Opt. Lett.* 29(18): 2184–2186.

Jullien, A., Canova, L., Albert, O., Boschetto, D., Antonucci, L., Cha, Y.-H., Rousseau, J., Chaudet, P., Chriaux, G., Etchepare, J., Kourtev, S., Minkovski, N. & Saltiel, S. (2007). Spectral broadening and pulse duration reduction during cross-polarized wave generation: influence of the quadratic spectral phase, *Appl. Phys. B* 87: 595–601.

Jullien, A., Chen, X., Ricci, A., Rousseau, J.-P., Lopez-Martens, R., Ramirez, L., Papadopoulos, D., Pellegrina, A., Druon, F. & Georges, P. (2010). High-fidelity front-end for high-power, high temporal quality few-cycle lasers, *Appl. Phys. B* pp. 1–6.

Jullien, A., Durfee, C., Trisorio, A., Canova, L., Rousseau, J.-P., Mercier, B., Antonucci, L., Chriaux, G., Albert, O. & Lopez-Martens, R. (2009). Nonlinear spectral cleaning

of few-cycle pulses via cross-polarized wave (xpw) generation, *Appl. Phys. B* 96: 293–299.

Jullien, A., Kourtev, S., Albert, O., Chriaux, G., Etchepare, J., Minkovski, N. & Saltiel, S. (2006b). Highly efficient temporal cleaner for femtosecond pulses based on cross-polarized wave generation in a dual crystal scheme, *Appl. Phys. B* 84: 409–414.

Jullien, A., Rousseau, J.-P., Mercier, B., Antonucci, L., Albert, O., Chériaux, G., Kourtev, S., Minkovski, N. & Saltiel, S. M. (2008). Highly efficient nonlinear filter for femtosecond pulse contrast enhancement and pulse shortening, *Opt. Lett.* 33(20): 2353–2355.

Kalashnikov, M. P., Risse, E., Schönnagel, H., Husakou, A., Herrmann, J. & Sandner, W. (2004). Characterization of a nonlinear filter for the front-end of a high contrast double-CPA Ti:sapphire laser, *Opt. Expr.* 12(21): 5088–5097.

Kalashnikov, M. P., Risse, E., Schönnagel, H. & Sandner, W. (2005). Double chirped-pulse-amplification laser: a way to clean pulses temporally, *Opt. Lett.* 30(8): 923–925.

Kapteyn, H. C., Murnane, M. M., Szoke, A. & Falcone, R. W. (1991). Prepulse energy suppression for high-energy ultrashort pulses using self-induced plasma shuttering, *Opt. Lett.* 16(7): 490.

Kiriyama, H., Michiaki, M., Nakai, Y., Shimomura, T., Sasao, H., Tanaka, M., Ochi, Y., Tanoue, M., Okada, H., Kondo, S., Kanazawa, S., Sagisaka, A., Daito, I., Wakai, D., Sasao, F., Suzuki, M., Kotakai, H., Kondo, K., Sugiyama, A., Bulanov, S., Bolton, P. R., Daido, H., Kawanishi, S., Collier, J. L., Hernandez-Gomez, C., Hooker, C. J., Ertel, K., Kimura, T. & Tajima, T. (2010). High-spatiotemporal-quality petawatt-class laser system, *Appl. Opt.* 49(11): 2105–2115.

Kiriyama, H., Michiaki, M., Nakai, Y., Shimomura, T., Tanoue, M., Akutsu, A., Kondo, S., Kanazawa, S., Okada, H., Motomura, T., Daido, H., Kimura, T. & Tajima, T. (2008). High-contrast, high-intensity laser pulse generation using a nonlinear preamplifier in a ti:sapphire laser system, *Opt. Lett.* 33(7): 645–647.

Kleinman, D. A. (1968). Theory of optical parametric noise, *Phys. Rev.* 174(3): 1027–1041.

Krausz, F. & Ivanov, M. (2009). Attosecond physics, *Rev. Mod. Phys.* 81(1): 163–234.

Kruer, W. L. (1988). *The Physics of Laser Plasma Interactions*, Addison-Wesley, Redwood City, CA.

Lévy, A., Ceccotti, T., D'Oliveira, P., Réau, F., Perdrix, M., Quéré, F., Monot, P., Bougeard, M., Lagadec, H., Martin, P., Geindre, J.-P. & Audebert, P. (2007). Double plasma mirror for ultrahigh temporal contrast ultraintense laser pulses, *Opt. Lett.* 32(3): 310–312.

Liu, J. & Kobayashi, T. (2010). Temporal contrast improvement of femtosecond pulses by a self-diffraction process in a kerr bulk medium. Frontiers in Optics 2010, Rochester, NY, USA, October 24-28 2010.

Lozhkarev, V. V., Freidman, G. I., Ginzburg, V. N., Katin, E. V., Khazanov, E. A., Kirsanov, A. V., Luchinin, G. A., Mal'shakov, A. N., Martyanov, M. A., Palashov, O. V., Poteomkin, A. K., Sergeev, A. M., Shaykin, A. A. & Yakovlev, I. V. (2006). Compact 0.56 petawatt laser system based on optical parametric chirped pulse amplification in kd*p crystals, *Opt. Expr.* 14(1): 446–454.

Lozhkarev, V. V., Freidman, G. I., Ginzburg, V. N., Katin, E. V., Khazanov, E. A., Kirsanov, A. V., Luchinin, G. A., Mal'shakov, A. N., Martyanov, M. A., Palashov, O. V., Poteomkin, A. K., Sergeev, A. M., Shaykin, A. A. & Yakovlev, I. V. (2007). Compact 0.56 petawatt laser system based on optical parametric chirped pulse amplification in kd*p crystals, *Laser Phys. Lett.* 4(6): 421–427.

Luan, S., Hutchinson, M. H. R., Smith, R. A. & Zhou, F. (1993). High dynamic range third-order correlation measurement of picosecond laser pulse shapes, *Meas. Sci. Technol.* 4(12): 1426–1429.

Major, Z., Trushin, S. A., Ahmad, I., Siebold, M., Wand, C., Klingebiel, S., Wa, T., Fülöp, T., Henig, A., Kruber, S., Weingartner, R., Popp, A., Osterhoff, J., Hörlein, R., Hein, J., Pervak, V., Apolonski, A., Krausz, F. & Karsch, S. (2009). Basic concepts and current status of the petawatt field synthesizer – a new approach to ultrahigh field generation, *Rev. Laser Eng.* 37(6): 431–436.

Marcinkevičius, A., Tommasini, R., Tsakiris, G., Witte, K. J., Gaizauskas, E. & Teubner, U. (2004). Frequency doubling of multi-terawatt femtosecond pulses, *Appl. Phys. B* 79(5): 547–554.

Minkovski, N., Petrov, G. I., Saltiel, S. M., Albert, O. & Etchepare, J. (2004). Nonlinear polarization rotation and orthogonal polarization generation experienced in a single-beam configuration, *J. Opt. Soc. Am. B* 21(9): 1659–1664.

Minkovski, N., Saltiel, S. M., Petrov, G. I., Albert, O. & Etchepare, J. (2002). Polarization rotation induced by cascaded third-order processes, *Opt. Lett.* 27(22): 2025–2027.

Moncur, N. K. (1977). Plasma spatial filter, *Appl. Opt.* 16: 1449–1451.

Monot, P., Doumy, G., Dobosz, S., Perdrix, M., D'Oliveira, P., Quéré, F., Réau, F., Martin, P., Audebert, P., Gauthier, J.-C. & Geindre, J.-P. (2004). High-order harmonic generation by nonlinear reflection of an intensehigh-contrast laser pulse on a plasma, *Opt. Lett.* 29(8): 893–895.

Nomura, Y. (2008). *Temporal characterization of harmonic radiation generated by intense laser-plasma interaction*, PhD thesis, Ludwig-Maximilians-Universität, München, Germany.

Nomura, Y., Veisz, L., Schmid, K., Wittmann, T., Wild, J. & Krausz, F. (2007). Time-resolved reflectivity measurements on a plasma mirror with few-cycle laser pulses, *New J. Phys.* 9(1): 9.

Osvay, K., Canova, L., Durfee, C., Kovács, A. P., Börzsönyi, A., Albert, O. & Lopez-Martens, R. (2009). Preservation of the carrier envelope phase during cross-polarized wave generation, *Opt. Express* 17(25): 22358–22365.

Pirozhkov, A. S., Choi, I. W., Sung, J. H., Lee, S. K., Yu, T. J., Jeong, T. M., Kim, I. J., Hafz, N., Kim, C. M., Pae, K. H., Noh, Y.-C., Ko, D.-K., Lee, J., Robinson, A. P. L., Foster, P., Hawkes, S., Streeter, M., Spindloe, C., McKenna, P., Carroll, D. C., Wahlström, C.-G., Zepf, M., Adams, D., Dromey, B., Markey, K., Kar, S., Li, Y. T., Xu, M. H., Nagatomo, H., Mori, M., Yogo, A., Kiriyama, H., Ogura, K., Sagisaka, A., Orimo, S., Nishiuchi, M., Sugiyama, H., Esirkepov, T. Z., Okada, H., Kondo, S., Kanazawa, S., Nakai, Y., Akutsu, A., Motomura, T., Tanoue, M., Shimomura, T., Ikegami, M., Daito, I., Kando, M., Kameshima, T., Bolton, P., Bulanov, S. V., Daido, H. & Neely, D. (2009). Diagnostic of laser contrast using target reflectivity, *Appl. Phys. Lett.* 94(24): 241102.

Renault, A., Augé-Rochereau, F., Planchon, T., D'Oliveira, P., Auguste, T., Chériaux, G. & Chambaret, J.-P. (2005). ASE contrast improvement with a non-linear filtering Sagnac interferometer, *Opt. Commun.* 248(4–6): 535–541.

Roskos, H., Seilmeier, A., Kaiser, W. & Harvey, J. D. (1987). Efficient high-power optical pulse compression with logarithmic wing analysis, *Opt. Commun.* 61(1): 81–86.

Schmid, K., Veisz, L., Tavella, F., Benavides, S., Tautz, R., Herrmann, D., Buck, A., Hidding, B., Marcinkevicius, A., Schramm, U., Geissler, M., Meyer-ter Vehn, J., Habs, D. & Krausz, F. (2009). Few-cycle laser-driven electron acceleration, *Phys. Rev. Lett.* 102(12): 124801.

Shah, R. C., Johnson, R. P., Shimada, T., Flippo, K. A., Fernandez, J. C. & Hegelich, B. M.

(2009). High-temporal contrast using low-gain optical parametric amplification, *Opt. Lett.* 34(15): 2273–2275.

Strickland, D. & Mourou, G. (1985). Compression of amplified chirped optical pulses, *Opt. Commun.* 56(3): 219–221.

Stuart, B. C., Feit, M. D., Herman, S., Rubenchik, A. M., Shore, B. W. & Perry, M. D. (1996). Nanosecond-to-femtosecond laser-induced breakdown in dielectrics, *Phys. Rev. B* 53(4): 1749–1761.

Stuart, B. C., Feit, M. D., Rubenchik, A. M., Shore, B. W. & Perry, M. D. (1995). Laser-induced damage in dielectrics with nanosecond to subpicosecond pulses, *Phys. Rev. Lett.* 74(12): 2248–2251.

Tavella, F., Schmid, K., Ishii, N., Marcinkevičius, A., Veisz, L. & Krausz, F. (2005). High-dynamic range pulse-contrast measurements of a broadband optical parametric chirped-pulse amplifier, *Appl. Phys. B* 81(6): 753–756.

Teisset, C., Ishii, N., Fuji, T., Metzger, T., Köhler, S., Holzwarth, R., Baltuška, A., Zheltikov, A. & Krausz, F. (2005). Soliton-based pump-seed synchronization for few-cycle opcpa, *Opt. Express* 13(17): 6550–6557.

Thaury, C., Quere, F., Geindre, J.-P., Levy, A., Ceccotti, T., Monot, P., Bougeard, M., Reau, F., d/'Oliveira, P., Audebert, P., Marjoribanks, R. & Martin, P. (2007). Plasma mirrors for ultrahigh-intensity optics, *Nature Phys.* 3: 424–429.

Tien, A.-C., Backus, S., Kapteyn, H., Murnane, M. & Mourou, G. (1999). Short-pulse laser damage in transparent materials as a function of pulse duration, *Phys. Rev. Lett.* 82(19): 3883–3886.

Tsakiris, G. D., Eidmann, K., Meyer-ter Vehn, J. & Krausz, F. (2006). Route to intense single attosecond pulses, *New J. Phys.* 8(1): 19.

Verhoef, A.-J., Seres, J., Schmid, K., Nomura, Y., Tempea, G., Veisz, L. & Krausz, F. (2006). Compression of the pulses of a Ti:sapphire laser system to 5 femtoseconds at 0.2 terawatt level, *Appl. Phys. B* 82(4): 513–517.

von der Linde, D., Sokolowski-Tinten, K. & Bialkowski, J. (1997). Laser-solid interaction in the femtosecond time regime, *Appl. Surf. Sci.* 109-110: 1 – 10.

Witte, S., Zinkstok, R. T., Wolf, A. L., Hogervorst, W., Ubachs, W. & Eikema, K. S. E. (2006). A source of 2 terawatt, 2.7 cycle laser pulses based on noncollinear optical parametric chirped pulse amplification, *Opt. Express* 14(18): 8168–8177.

Wittmann, T., Geindre, J. P., Audebert, P., Marjoribanks, R., Rousseau, J. P., Burgy, F., Douillet, D., Lefrou, T., Ta Phuoc, K. & Chambaret, J. P. (2006). Towards ultrahigh-contrast ultraintense laser pulses—complete characterization of a double plasma-mirror pulse cleaner, *Rev. Sci. Instrum.* 77: 083109.

Yanovsky, V., Chvykov, V., Kalinchenko, G., Rousseau, P., Planchon, T., Matsuoka, T., Maksimchuk, A., Nees, J., Cheriaux, G., Mourou, G. & Krushelnick, K. (2008). Ultra-high intensity- 300-tw laser at 0.1 hz repetition rate, *Opt. Express* 16(3): 2109–2114.

Yuan, P., Xie, G., Zhang, D., Zhong, H. & Qian, L. (2010). High-contrast near-ir short pulses generated by a mid-ir optical parametric chirped-pulse amplifier with frequency doubling, *Opt. Lett.* 35(11): 1878.

Ziener, Ch., Foster, P. S., Divall, E. J., Hooker, C. J., Hutchinson, M. H. R., Langley, A. J. & Neely, D. (2002). Specular reflectivity of plasma mirrors as a function of intensity, pulse duration, and angle of incidence, *J. Appl. Phys.* 93: 768.

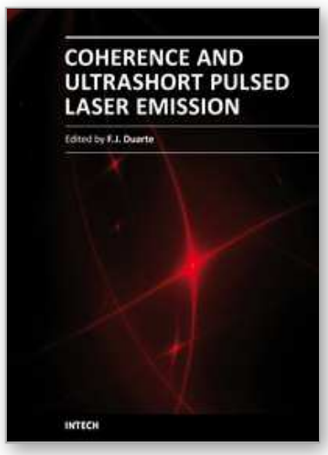

Coherence and Ultrashort Pulse Laser Emission

Edited by Dr. F. J. Duarte

ISBN 978-953-307-242-5
Hard cover, 688 pages
Publisher InTech
Published online 30, November, 2010
Published in print edition November, 2010

In this volume, recent contributions on coherence provide a useful perspective on the diversity of various coherent sources of emission and coherent related phenomena of current interest. These papers provide a preamble for a larger collection of contributions on ultrashort pulse laser generation and ultrashort pulse laser phenomena. Papers on ultrashort pulse phenomena include works on few cycle pulses, high-power generation, propagation in various media, to various applications of current interest. Undoubtedly, Coherence and Ultrashort Pulse Emission offers a rich and practical perspective on this rapidly evolving field.

InTech Europe
University Campus STeP Ri
Slavka Krautzeka 83/A
51000 Rijeka, Croatia
Phone: +385 (51) 770 447
Fax: +385 (51) 686 166
www.intechopen.com

InTech China
Unit 405, Office Block, Hotel Equatorial Shanghai
No.65, Yan An Road (West), Shanghai, 200040, China
中国上海市延安西路65号上海国际贵都大饭店办公楼405单元
Phone: +86-21-62489820
Fax: +86-21-62489821

IntechOpen